Science on Form: Proceedings of the First International Symposium for Science on Form,
General Editor: S. Ishizaka, Editors: Y. Kato, R. Takaki, and J. Toriwaki, 113-120.

Cellular Automata and Chaos in N-equivalent Switching Elements

Kazunori Aoki and Nobumichi Mugibayashi

Department of Electrical Engineering, Faculty of Engineering, Kobe University, Rokkodai, Nada, Kobe 657, Japan

Keywords: Cellular Automata, coupled chaos, symbolic soliton

Cellular automata and coupled chaos have been investigated in one-dimensional lattice chain of N-equivalent switching elements. A switching element shows the bistability and behaves like a random nerve net. The firing activity S_t of each element takes one of the symbolic states of 1 or 0 in accord with $S_t \geq 0.5$ or $S_t < 0.5$, respectively. The evolution of the symbols exhibits rich structures of cellular automata for several types of local interaction. According to Wolfram, classes 1,2 and 3 are frequently observed. Spatial period doubling of the growing elements, running modes of the symbolic solitons, interference of the solitons, and the bifurcations of the classes are presented.

INTRODUCTION

Cellular automata have been widely proposed as computational tools to study the complex nature such as self-reproduction, evolution of organization in biology and flip-flop of the lattice spins in the Ising model (e.g., Vichniac:1984). In one-dimensional (1D) cellular automata, 1D lattice chain is composed of simple identical components, where each component has a value of 1 or 0 and interacts with the neighbourhood (Wolfram:1984). Symbolic representation of the lattice dynamics in a couple of iterative map equations is expected to develope cellular automata if each component of the lattice has one of two symbolic states. In general, a switching element or a bistable element takes either one of two symbols of on- and off-states. Our special concern is in the field of nonlinear networks; there is a trend to understand the information handling structures in the nonlinear networks such as extended computor system and neural network system by means of cellular automata (Choi & Huberman:1983, Huberman:1985). In this paper, motivated by the recent elavorated works, we investigate the global dynamics of cellular automata and coupled chaos developed in 1D lattice chain of N-equivalent switching elements.

DESCRIPTION OF THE MODEL

A couple of the iterative map equations are proposed as follows

$$S^i_{t+1} = F(-4S^i_t + 2 - R \sin(2\pi S^i_t) - T f(S^{i-1}_t, S^{i+1}_{t-1})), \quad (1)$$

$$F(y) = (1 + \tanh(y))/2 , \quad (2)$$

where S^i_t is the order parameter of the i-th element (i=1,2..N) at discrete time t, R and T are control parameters, and function f denotes the local interactions with the nearest neighbours. Each element corresponds to a McCullough-Pitts random nerve net with the firing activity $S^i_t \in I=[0,1]$ (Amari:1974). With T=0, function F in Eqs.(1) and (2) has the following properties (Aoki et al.: 1984) as a function of R;

(A) $0 \lesssim R \lesssim 1/\pi$, $\bar{S}=0.5$ is unstable and S_t is oscillatory with period 2.
(B) $1/\pi < R \lesssim 3/\pi$, $\bar{S}=0.5$ is stable equilibrium point.
(C) $3/\pi < R \lesssim 1.387$, $\bar{S}$ is unstable and S_t shows the bistability.
(D) $R > 1.387$, S_t shows period doubling bifurcation route to chaos.

If S_{t+1} and S_t are replaced by $\bar{S}$ in Eq. (1), we can construct a catastrophe curve which is a section of the folded manifold of Riemann-Hugoniot type catastrophe by Thom:1975. Solid line in Fig.1 shows the catastrophe curve $\bar{S}=F(\bar{S},R)$ which satisfies the condition of a conflict strutum. Properties (B) and (C) directly result from the catastrophe curve and properties (A) and (D) are related with the destabilization of the equilibrium points in Eq. (1).

When N-equivalent switching elements are coupled ($T \neq 0$), properties in (A)-(D) mentioned above no longer hold for any values of R, since each element always suffers the local stimuli from the nearest neighbours. In the coupled lattice map, the firing activity S^i_t exhibits the chaotic motion trapped in either one of two basins of attraction which form a symmetric pair around $\bar{S}=0.5$. In accord with $S^i_t \geq 0.5$ or $S^i_t < 0.5$, two symbols 1(↑) or 0(↓) are defined, respectively.

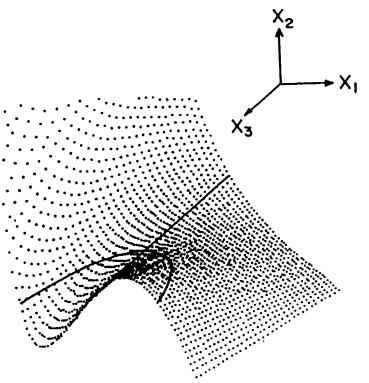

Fig.1 Folded manifold of Riemann-Hugoniot type catastrophe of the algebraic set $U=\{(x_1,x_2,x_3) \in R^3\}$, where $x_1=F(x_1x_2+2-x_3\sin(2\pi x_1))$, and x_1 and x_3 correspond to $\bar{S}$ and R, respectively. Solid line is a section of the folded manifold at $x_2=-4$.

RESULTS AND DISCUSSIONS

In this paper, we investigate the cellular automata with the following rules of the local interactions

$$f^a = \sin(4\pi S^{i-1}_t) , \quad (3)$$

$$f^b = \sin(2\pi(S^{i-1}_t + S^{i+1}_{t-1}) + \phi) , \quad (4)$$

$$f^c = \sin(2\pi S_t^{i-1} + \phi)\ \sin(2\pi S_{t-1}^{i+1} + \phi)\ , \qquad (5)$$

where ϕ is the phase lag. We describe the global dynamics of the spatial period doubling of the growing elements, running modes of the symbolic solitons, interference of the solitons, and bifurcations of the classes.

1. Spatial period doubling of growing elements.

Let us consider one way coupling of N-switching elements with the local interaction f^a, in which values of control parameter R grow by R(i+1)=R(i)+ΔR (i=1,2..N). It may describe an artificial model of some kind of self-reproduction in the nonlinear networks. Fig.2 shows the firing activities of N-switching elements as a function of R(i) with T=0.2, R(1)=0.9, R(600)=1.5, ΔR=0.001, and N=600. In the course of the growth, S_t^i shows 2^k spatial doubling as a function of R(i). Not clearly seen in the figure, but it is to be noted that the symbolic configuration of the growing elements is 101010.. , in the range $0.9 \lesssim R(i) \lesssim 1.18$. Namely, if the j-th element is trapped in a basin of attraction with 2^k-period cycle and takes a symbol 1, then the next element is trapped in another basin of attraction with the same period and takes the symbol 0, and so on. With further growth of the elements, 2^k-period cycle bifurcates successively into chaotic motions, but the elements keep the

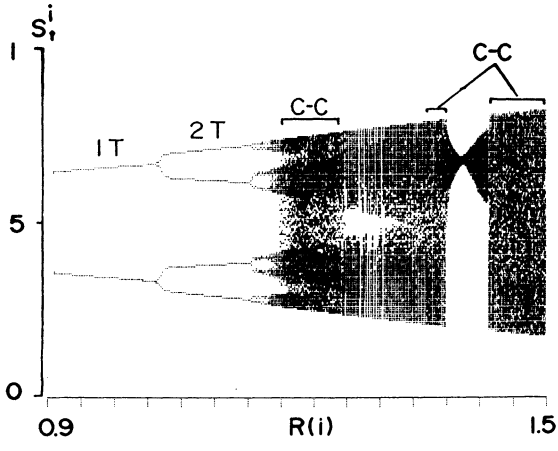

Fig.2 Bifurcation diagram of the firing activities of the growing elements as a function of R(i). After the initial transients, the firing activities with t=800∿1000 are plotted.

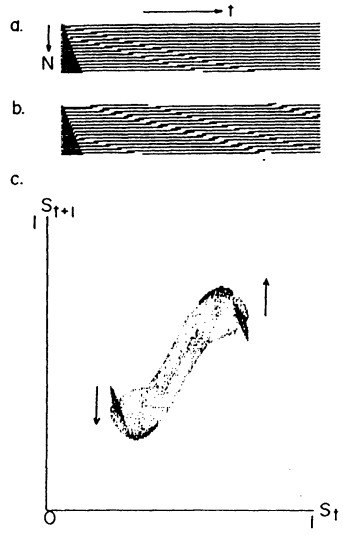

Fig.3 Running modes of the symbolic solitons in (a) linear lattice chain, (b) looped lattice chain, with N=31, and iterations up to t=300, and (c) the iterative mapping of the firing activity of the 15th element in (b), with t=300∿5000. Control parameters are; T=0.2, R=1.2. In (a)∿(c), the initial states are chosen to be S_0^i=0.056. There is sensitive dependence on initial states. f^a must be taken into account from 1st iterate.

symbolic configuration 101010... With $0.9 \lesssim R(i) \lesssim 1.38$ and $1.43 \lesssim R(i) \lesssim 1.5$, the bifurcation diagram is symmetric around $\bar{S}=0.5$. In several regions, denoted by C-C, the elements show flip-flop jumps from a basin of attraction to another, i.e., chaos-chaos transition (Aizawa:1982). In the range of $1.38 \lesssim R(i) \lesssim 1.43$, the bifurcation diagram is symmetry-broken. Detailed descriptions will be reported elsewhere.

2. Running modes of the symbolic solitons.

With a rule f^a, the symbolic domains of the initial disorder run through the lattice chain. Fig.3 shows the cellular automata of N=31 elements in a linear lattice chain (a), and a looped lattice chain (b), respectively. For the linear lattice chain, the symbolic domains formed by the initial disorder disappear at the N-th element and the final symbolic configuration is 0101..010. For the looped lattice chain, the symbolic domains keep the running modes. The propagation of the symbolic domain is quite similar to the soliton propagation in 1D molecular electron devices by Carter:1984. A symbolic mismatch $\tilde{1}$ of the i-th element in a configuration of 0101...01$\tilde{1}$0101.. at time t flips to 0 at $t+\ell$, $\tilde{0}$ of the (i+1)-th element to 1 at t+m, $\tilde{1}$ of the (i+2)-th element to 0 at t+n and so on, where velocity of the symbolic soliton is given by $v_s=2/(n-\ell)$. At T=0.2, the propagation of the symbolic solitons in a looped lattice chain is observable only with $0.66 \lesssim R \lesssim 1.21$ under the initial states specified in Fig. 3. The velocity increases with decreasing R; $v_s=15/117$ at R=1.2 and $v_s=1$ at R=0.68. At $R \sim 0.65$, the homogeneous configuration oscillates with period 2 by 111...111→000...000→. With $1.21 < R \lesssim 1.38$, the initial disorder 110100..11001 keep a class 2 cellular automaton.

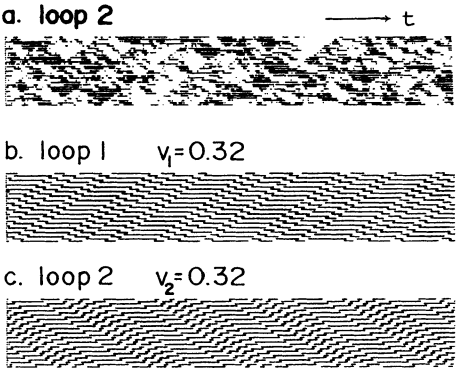

Fig.4 (a) Interference pattern of the solitons in loop 2, (b) running modes of the solitons in loop 1, and (c) running modes of solitons in loop 2 without the perturbation. Control parameters are; R=1.1, T=0.2 for both loops. t=0∿380.

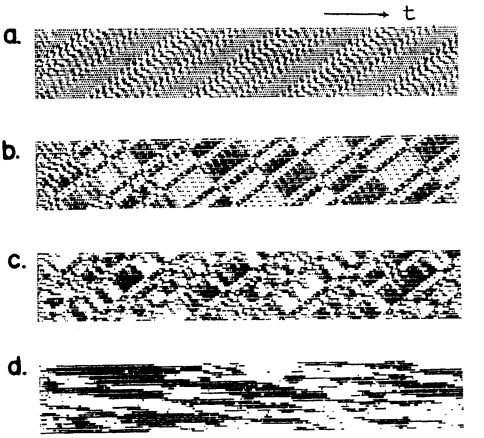

Fig.5 Change of the interference patterns of the solitons in loop 2 as a function of the velocity ratio v_2/v_1; (a) 2.5, (b) 2.2, (c) ~1 and (d) 0.4, respectively, where v_1=0.32. t=0∿350.

With R>1.38, cellular automata reveal chaotic patterns.

In progress of a cellular automaton, the firing activity of each element exhibits chaotic motion. Fig.3c shows the iterative mapping of the firing activity of the 15th element in a N=31 looped lattice chain. Chaotic motion is trapped in a basin of attraction ↑(or ↓), but jumps to another basin of attraction ↓(or ↑) whenever the symbolic soliton passes through the element. The flip-flop jump process is qualitatively explained by virtue of Riemann-Hugoniot catastrophe (cf. Fig.1). Two symmetric potential minima in a conflict strutum form two symmetric basins of attraction which are discriminated by some potential barrier(Thom :1975). The chaotic motion trapped in a basin of attraction jumps to another basin of attraction if the fluctuating force from the nearest neighbour is sufficiently large. The velocity of the soliton is expected to increase by reducing the potential barrier height and thus by decreasing the value of control parameter R. Kaneko:1986 has reported different kind of the soliton propagation in coupled logistic lattice, which will appear in this issue.

3. Interference of the solitons.

As an application of the solitons propagation, let us consider the soliton dynamics of a looped lattice chain (loop 2) perturbed by the solitons propagation in another looped lattice chain (loop 1). The proposed map equations are;

$$\text{loop 1 : } \tilde{S}^{i}_{t+1} = F(-4\tilde{S}^{i}_{t} + 2 - \tilde{R}\sin(2\pi\tilde{S}^{i}_{t}) - \tilde{T}\, f^{a}(\tilde{S}^{i+1}_{t})), \qquad (6)$$

$$\text{loop 2 : } S^{i}_{t+1} = F(-4S^{i}_{t} + 2 - R\sin(2\pi S^{i}_{t}) - T\, f(S^{i-1}_{t}, \tilde{S}^{i+1}_{t})), \qquad (7)$$

$$\text{and} \quad f(S^{i-1}_{t}, \tilde{S}^{i+1}_{t}) = \sin(4\pi(S^{i-1}_{t} + \tilde{S}^{i+1}_{t})),$$

where i=1,2..N, and entities in loop 1 is denoted by tilde. If $\tilde{S}^{i+1}_{t}=0$ in f of Eq.(7), then solitons in loops 1 and 2 propagate independently in the opposite direction with the velocities v_1 and v_2, respectively. Fig.4 shows (a) a typical example of the interference pattern of the solitons in loop 2, and (b),(c) the running modes of the solitons in loops 1 and 2, respectively, where N=31. In Figs.4∿6, all the initial states are weakly randomized by $S^{i}=\tilde{S}^{i}_{o}=0.214+\xi^{i}$, $|\xi^{i}|<0.013$, where ξ^{i} are random variables. Fig.5 shows change of the interference patterns of the

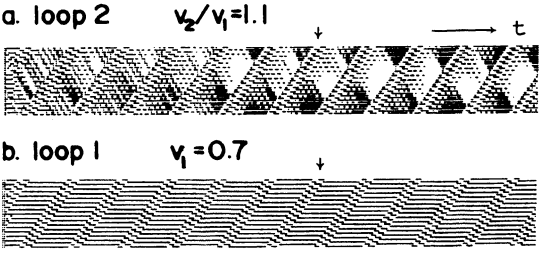

Fig.6 (a) Interference pattern of the solitons in loop 2, and(b)running modes of solitons in loop 1. Control parameters are; T=$\tilde{T}$=0.2, R=0.8, and $\tilde{R}$=0.9. The iterations were done up to t=445.

solitons in loop 2 as a function of the velocity ratio v_2/v_1. There appear regular interference patterns in a, b; several domains run through the lattice with velocity v_1 in a, and rectangular tile pattern is seen in b. By decreasing the velocity ratio, the tile patterns bifurcate to irregular or chaotic patterns with $v_2/v_1 \lesssim 1$. In Fig.5d, fully developed turbulence is clearly shown. Fig.6a shows another example of the interference pattern in loop 2, in which traces of the running modes of loop 1 are observed, as indicated by arrows. Although there is no room to discuss the mechanism of the formation of the interference pattern in detail, it is briefly to be noted that the presented results give a new regime of the soliton dynamics in the cellular automata.

4. Bifurcations of the classes.

With interaction rules f^b and f^c, a variety of cellular automata are observed, which are classified into classes 1, 2 and 3 cellular automata. According to Wolfram:1984, we briefly mention about the classes. Class 1 cellular automata evolve after a number of time steps from almost all initial states to a unique homogeneous state, all sites having the same value. Class 2 cellular automata exhibit stational symbolic series of which configurations depend on the control parameters and also on the initial states. In some cases, a few lattice sites in a configuration oscillate periodically. Class 3 cellular automata exhibit aperiodic or chaotic patterns for almost all initial states.

In Fig.7, the cellular automata with rule f^b are shown as a function of T with fixed values of R=1 and $\phi=2\pi/3.5$. The initial conditions are weakly randomized. With $T\lesssim 0.1$, cellular automata look like class 1, but symbol 1 is persistent at the boundaries of the linear lattice chain (N=90),i.e., class 2, as is shown in Fig.7a. For class 2 cellular automata, the symbolic configuration is divided into several territories (Fig.7b,c) of 0101..01. Bifurcation from class 2 to class 3 cellular automata occurs at T=0.16. With $0.16\lesssim T\lesssim 0.235$, chaotic patterns are also bound in the territories (Fig.7d). A few lattice sites at a boundary between two territories always suffer the local stimuli from both sides of the territories. If the local stimuli are not sufficiently large, firing activities of the lattice sites stay in one basin of attraction. Therefore, chaotic patterns do not diffuse outside the boundary, and informations are stocked in each territory. With $T\gtrsim 0.235$, chaotic patterns diffuse through the boundaries. The developed turbulence in Fig.7 -e,f indicates the procession of the informations throughout the lattice chain.

Bifurcation from class 1 to class 2 cellular automata is also observed in the different region of the control parameters. With R=1 and T=0.22, class 1 cellular automata of symbol 1 are stable in the range of $2\pi/2.921\lesssim\phi\lesssim 2\pi/1.59$ and bifurcate to class 2 cellular automata with $\phi\lesssim 2\pi/2.921$. With $\phi\lesssim 2\pi/3$, class 2 cellular automata bifurcate to class 3 (cf. Fig.7d).

In Fig.8, another example of cellular automata with rule f^c in the N=90 linear lattice chain is shown as a function of ϕ under the fixed values of R=1.12 and T=0.67. Dusty patterns of class 3 are observed with $\phi\lesssim -\pi/3.6$. In the range of $-\pi/3.21\lesssim\phi\lesssim -\pi/3.6$, nucleations of the dust occur in several regions at the initial stage of the iterations (Fig.8b), and the persistent

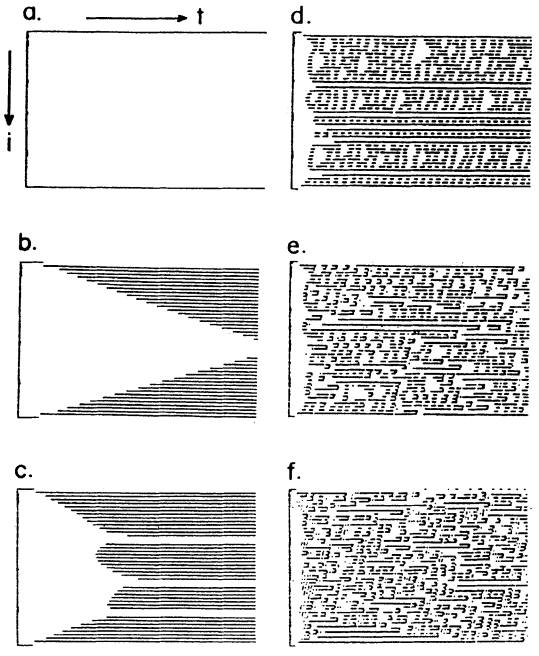

Fig.7 Cellular automata of rule f^b, with N=90, R=1 and $\phi=2\pi/3.5$. Values of T are; (a)0.1, (b)0.13, (c)0.14, (d)0.22, (e)0.25, and (f)0.28, respectively. The initial states are weakly randomaized by $S_o^i = 0.514 + \xi^i$, $|\xi^i| < 0.0138$. t=0∿300.

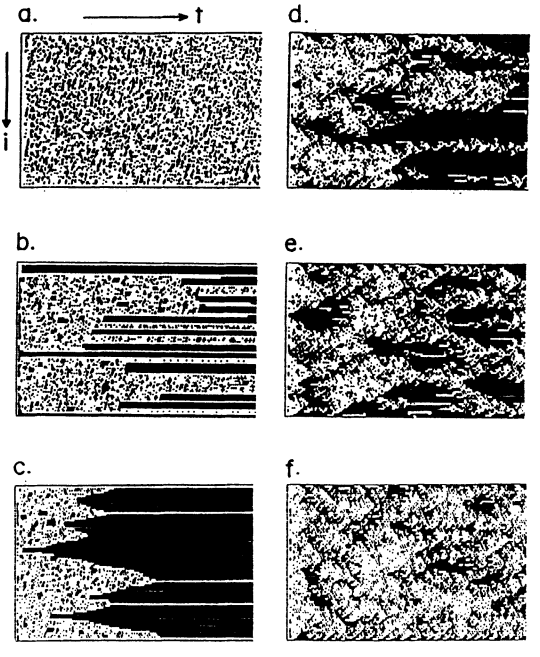

Fig.8 Cellular automata of rule f^c, with R=1.12 and T=0.67. Values of ϕ are; (a)$-\pi/2.5$, (b)$-\pi/3.5$, (c)$-\pi/3.7$, (d)$-\pi/4.95$, (e)$-\pi/5$ and (f)$-\pi/5.5$, respectively. The initial conditions are the same as those in Fig.7. t=0∿300.

series (e.g., llll) follows after each nucleation. The dusty pattern is bound in the territory. Class 2 cellular automata appear in the range of $-\pi/3.7 \lesssim \phi \lesssim -\pi/4.84$. After the dusty pattern has died out, several 0 sites surrouded by 1 sites are retained, as is shown in Fig.8c. With $\phi > -\pi/4.84$, class 2 cellular automata bifurcate to class 3 cellular automata of cloudy patterns (Fig.8d,e,f). Around the bifurcation point, the initial transients are long lived for both class 2 and 3 cellular automata. In Fig.8d, clouds are almost coalescent at $t \sim 300$, but never fall into class 2 cellular automaton with $t >> 300$.

CONCLUSION

Global dynamics of cellular automata in a lattice chain of N-equivalent switching elements which behave like nerve network have been investigated. Spatial period doubling of the growing elements, running modes of the symbolic solitons, interference of solitons, and the bifurcations of the classes are recognized. Chaotic motions of the firing activities are essentially important for the developement of cellular automata. For class 3 cellular automata, chaotic patterns of the symbols are caused by chaos-chaos transition of the firing activities. The 01 symmetry in cellular automata is assured by π-rotational symmetry of two basins of attraction. In any case of class 3 cellular automata, chaotic motions of the switching elements are cooperative, and the auto-regulation of a chaotic pattern in the symbolic dynamics is uniquely determined by a specific interaction rule, control parameters and initial conditions.

REFERENCES

Aizawa, Y. and Uezu, T. (1982): Global aspects of the dissipative dynamical systems. II. Prog. Theor. Phys.,68:1864.

Amari, S.I. (1974): A method of statistical neurodynamics. Kybernetik,14:201.

Aoki, K., Ikezawa, O. and Yamamoto, K. (1984): Bifurcation routes to chaos in the firing activity. Phys. Lett.,106A:343.

Carter, F.L. (1984): The molecular device computor:point of departure for large scale cellular automata. Physica,10D:175.

Choi, M.Y. and Huberman, B.A. (1983): Dynamic behavior of nonlinear networks. Phys. Rev.,28A:1204.

Huberman, B.A. (1985): Probabilistic cellular automata. Nonlinear phenomena in physics. [ed. F. Claro. New York, Springer-Verlag.]:129-137.

Kaneko, K. (1986): Spatio-temporal patterns in coupled map lattices. to be published in this issue., see also Kaneko, K. (1984): Prog. Theor. Phys.,72:480.

Vichniac, G.Y. (1984): Simulating physics with cellular automata. Physica,10D:96.

Wolfram, S. (1984): Universality and complexity in cellular automata. Physica,10D:1.